Earthquake Engineering, Tenth World Conference © 1992 Balkema, Rotterdam. ISBN 90 5410 060 5

Dynamic response of circular bridge piers

Larry L. Dodd & Nigel Cooke
University of Canterbury, Christchurch, New Zealand

ABSTRACT: Fourteen one-sixth scale model bridge piers were tested on a uni-directional shaking-table. The purpose of the tests was to determine whether analytical models which were developed from quasi-static tests, could adequately describe the response of piers in the dynamic situation associated with an earthquake. The results show that design rules developed from these models are more than adequate, and indicate that ductilities greater than six can be achieved easily and that flexural strengths are enhanced by the dynamic loading.

1 INTRODUCTION

The main purpose of the dynamic tests, see Dodd (1992), described in this paper was to check that the design rules for circular, reinforced concrete bridge piers, which were developed from static tests at the University of Canterbury over the last two decades, are adequate in the dynamic situation associated with an earthquake. The static tests have revealed the member load-deflection properties of circular piers with various amounts and configurationss of reinforcing steel. The findings have been used to develop and to confirm member hysteretic rules and the ductility capacity.

In an actual earthquake, the damaging loads on the piers are induced by the inertia of the portion of the structure which is being supported by the piers. The magnitude of these loads depends on the interaction between the ground motion and the structure. The response of the structure to the ground motion depends on the instantaneous stiffness of the structural elements, any additional flexibility in the system, and the characteristics of the ground motion.

The dynamic behaviour of the materials making up the member, such as strain rate dependence, can influence the response of the structure. Instability in the system when the member can no longer resist the inertial load during ground acceleration peaks must also be considered.

Shake-table tests on fourteen one-sixth scale, circular, reinforced concrete bridge piers were carried out. Sinusoidal and El Centro 1940N-S type table motions were used, and the pier responses were measured. The piers were all flexurally dominated designs, see Dodd and Cooke (1991), in order that shear failures would not develop.

2 PIER DETAILS AND EXPERIMENTAL TEST ARRANGEMENT

All piers were 200mm in diameter and contained the same quantity of longitudinal reinforcement (18 - 6mm diameter deformed bars with a measured yield stress of 450 MPa). The lateral reinforcement consisted of either a 4mm or 3.15mm diameter round bar as a spiral with a yield stress of 260 MPa and with different bar spacings. A concrete with an aggregate gradation similar to that of a full-scale concrete mix but truncated at a maximum size of 10mm was used. Concrete cylinder strengths of between 29 and 43MPa were achieved at the time of testing.

Piers with different aspect ratios were tested. Aspect ratios, which is the length of the pier divided by the diameter, of 4, 7 and 10 were chosen as being representative of typical flexurally dominated bridge piers in New Zealand. All of the piers exhibit the effects of P-Δ, but the taller piers are more prone to failure from instability resulting from P-Δ effects than the shorter ones. P-Δ effects are caused by the eccenticity of the inertial weight with respect to the base of the pier, resulting in additional bending moments to those in the piers introduced from the horizontal inertia forces.

Two axial load levels were used in these tests. The lowest axial load was obtained by manufacturing a five tonne concrete block and supporting it on the pier as shown in Figure 1. A stabilising strut was

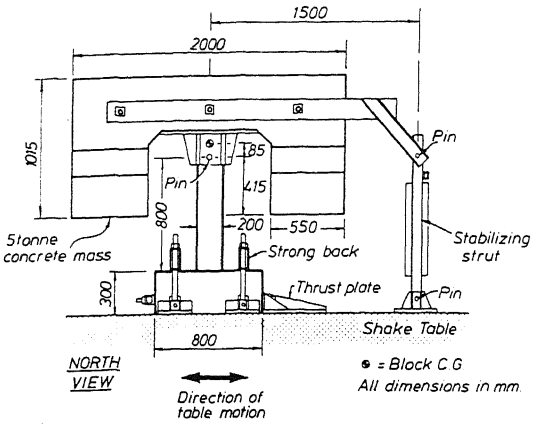

Figure 1. Experimental testing arrangement

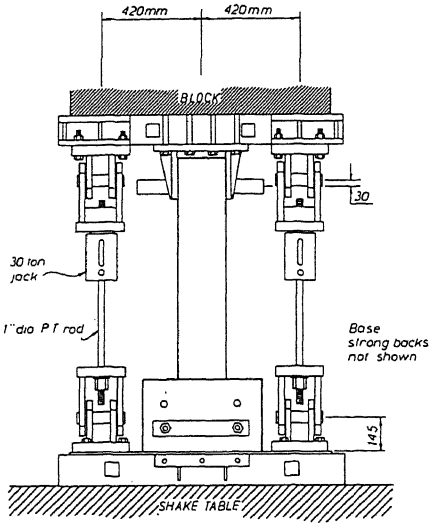

Figure 2. Vertical prestressing arrangement

provided to prevent the development of any rotational inertia and to support the block in a statically determinate manner. Loads in these struts were small, and did not greatly influence the magnitude of the axial load in the piers. The low axial load ratio, defined as the axial load in the pier, P, divided by the nominal strength of the concrete pier, $f'_c A_g$. where f'_c is the concrete strength and A_g is the gross cross sectional area of the pier, was approximately 0.05.

The high axial load ratio, representing the maximum practical ratio was obtained by increasing the axial load on the pier by the use of two vertical, external prestressing bars as shown in Figure 2.

Table 1 gives details of the axial load ratios and aspect ratios for each pier. Also given are the shake-table motion details. Piers were subjected to either a four cycle sinusoidal motion or to a motion based on the El Centro 1940N-S earthquake record. The actual table motion is modified by the limitations of the table, particularly the maximum velocity and the flexible connection between table and driving ram. However, these limitations did not interfere with the tests, and all piers were shaken to collapse.

Table 1. Specimen geometric and loading conditions

Pier Number	Axial Load Ratio	Aspect Ratio	Pier Length (mm)	Shaking Motion
1a	0.05	4	800	Sinusoidal
1b	0.05	4	800	El Centro
2a	0.05	7	1400	Sinusoidal
2b	0.05	7	1400	El Centro
3a	0.05	10	2000	Sinusoidal
3b	0.05	10	2000	El Centro
4	0.40	4	800	El Centro
5	0.40	7	1400	El Centro
6	0.40	10	2000	El Centro
7	0.05	4	800	El Centro
8	0.40	4	800	El Centro
9	0.05	7	1400	El Centro
10	0.05	4	800	El Centro
11	0.04	4	800	El Centro

3 TEST RESULTS

3.1 *Piers with low axial load*

The results presented here are only a very small part of the data obtained during the tests. Each pier was subjected to a number of shakes with increasingly larger demands made on them, and only parts of some of these shakes have been spliced together to give a clear representation of the results.

A typical spliced plot of table acceleration with time is shown in Figure 3. In this case, parts of eight records have been spliced to give a clear picture of lateral block inertia force versus block displacement, as in Figure 4. Pier 1b was subjected to El Centro, and Figure 4a shows the ratchet effect that can sometimes occur in an earthquake, where most of the displacement takes place in one direction. A member ductility of approximately eight was obtained, although the design was based on an estimated value of six.

Pier 1a was subjected to a four cycle sinusoidal motion and Figure 4b shows the approximately symmetrical response of this pier. Again, ductilities of eight were achieved,as for Pier 1b. The two straight lines are based on the flexural strength of the pier

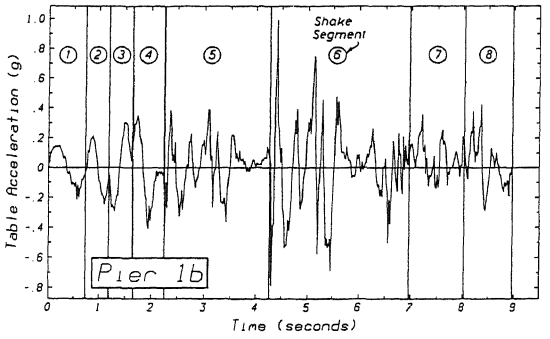

Figure 3. Pier 1b. Table acceleration versus time

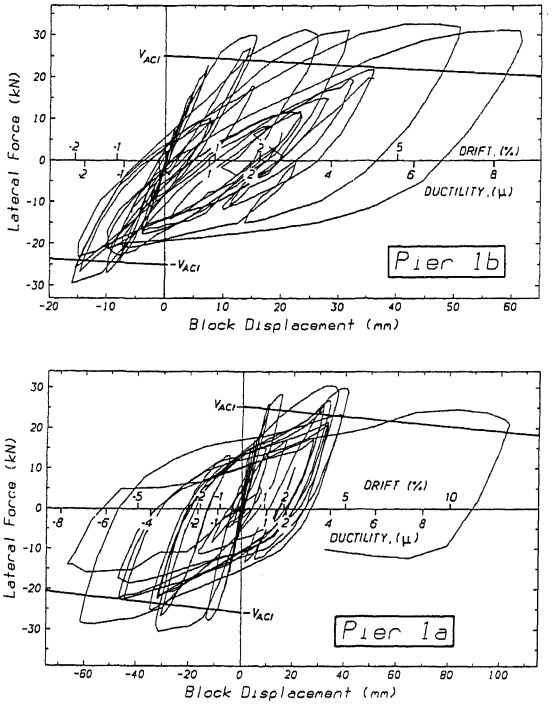

Figure 4. Lateral shear force versus block displacement for (a) Pier 1b and (b) Pier 1a

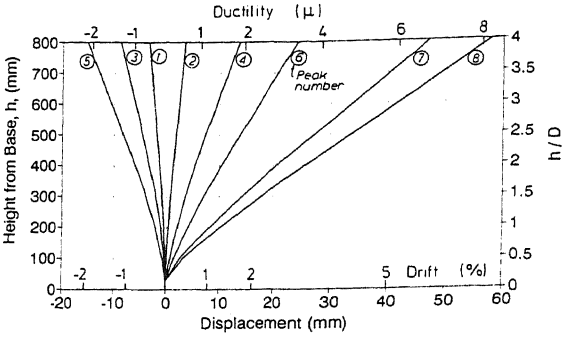

Figure 5. Pier 1b. Pier displacement for various shakes

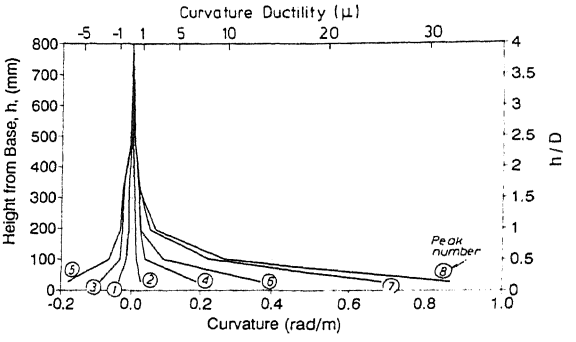

Figure 6. Pier 1b. Measured curvature for various shakes

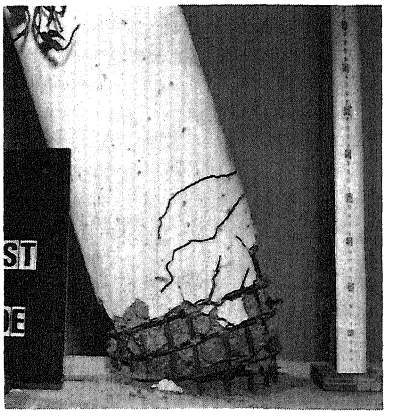

Figure 7. Hinge region of a Pier 10 at collapse

section being determined from the nominal strength calculation method in the American Concrete Institute 1983 Specification ACI318-83, to give the shear force V_{ACI}. The slope of the lines indicate the P-Δ influence on lateral shear force capacity.

As with all of the results, without exception, the maximum lateral shear force resisted by the piers is considerably greater than V_{ACI}. Static tests indicate a 13% - 20% increase in strength above V_{ACI}, due mainly to improved performance resulting from well confined hinge zones. Further overstrengths of between 10% to 20% can be attributed to the dynamic response of the materials, namely the strain rate sensitivity which leads to greater stress levels with greater rate of strain.

Figure 5 shows the displaced shape of the pier at peak displacements and member ductilities achieved and Figure 6 shows the distribution of curvature and

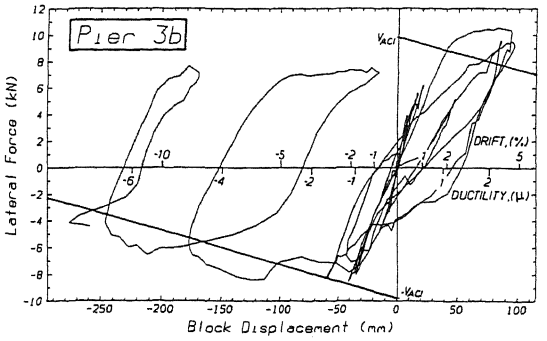

Figure 8. Pier 3b. Lateral shear force versus block displacement

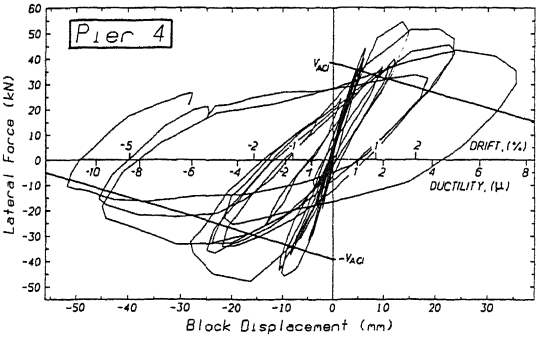

Figure 9. Pier 4. Lateral shear force versus block displacement

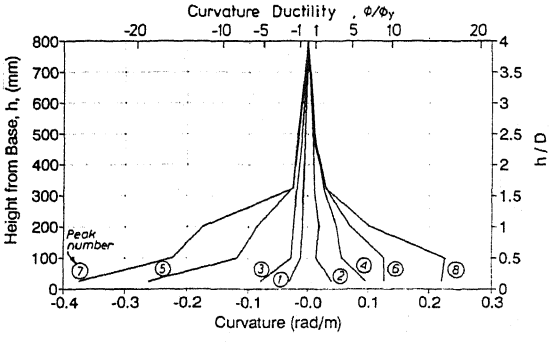

Figure 10. Pier 4. Measured curvature for various shakes

average section curvature ductilities achieved in each spliced record. Measured average curvature ductilities of over thirty are shown in Figure 6, with a region of plasticity extending over a length of 300 mm (h/D = 1.5, where h = 300mm and D is the pier diameter) but most of the plasticity occurs over a length of 100mm (h/D = 0.5). Figure 7 shows an excessively deformed hinge region adjacent to the base, and fractured longitudinal reinforcement brought about

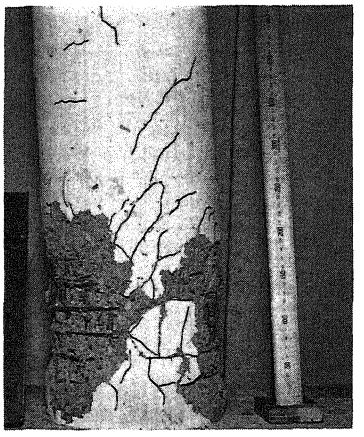

Figure 11. Hinge region of Pier 11 at collapse

by localised cracking associated with compression buckling followed by fracture on straightening of the bar in tension.

Piers with low axial loads and aspect ratios of seven also failed in the same manner as those piers just described. However, the tall piers did not fail. Figure 8 shows the load-deflection relationship for one of these piers. The loops are all stable and show a final negative drift of 13% at which point the test was stopped by preset buffers. The region of plasticity is greater than the other piers, extending over a length of 500mm (h/D = 2.5) with most of the deformation taking place over a length of 350mm (h/D = 1.75).

3.2 *Piers with high axial load*

Figure 9 is a plot of lateral load on the pier versus concrete block displacement for Pier 4, a short pier. It again shows that the ACI shear force is considerably exceeded and that the P-Δ effect also has a strong influence on behavioural response because of the high axial loads; ductilities of over ten were obtained. Failure is defined in New Zealand by strength falling below 80% of the peak strength. This occurs at ductilities of approximately seven, however, clearly the loops are stable after this point even though the strengths have fallen below the acceptable level. Figure 10 indicates that average section curvature ductilities of over 25 were measured and that although the region of plasticity extended over the same lengths as the piers with low axial load, large curvatures were measured away from the base. The reason for this is that the base block provides some local confinement and failure takes place away from the base as shown in Figure 11.

The piers with an aspect ratio of seven behaved in a very similar manner to the piers with an aspect ratio of four, just described. However, the tall piers

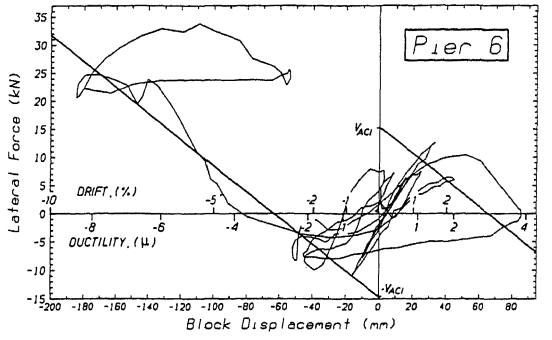

Figure 12. Pier 6. Lateral shear force versus block displacement

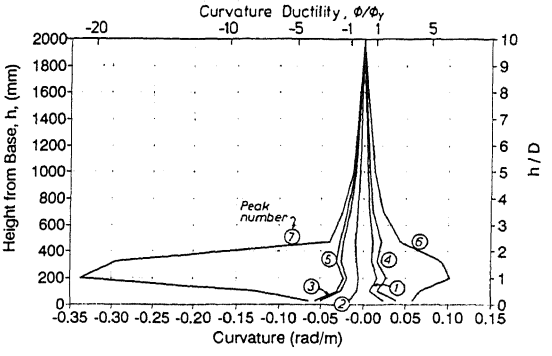

Figure 13. Pier 6. Measured curvature for various shakes

were influenced by instability resulting from P-Δ effects. Figures 12 and 13 show that collapse from instability took place at a ductility of +4 (not at -8) where the lateral shear force is zero. The length of the region of plasticity is greater than the shorter piers, and crushing of the concrete occurs at a distance of approximately 1.5 times the pier diameter, as in Figure 11.

4 CONCLUSIONS.

All piers performed satisfactorily. The performance of the piers subjected to low axial loads did not appear to be greatly influenced by the amount of confining steel. They failed as a result of fracture of the longitudinal steel, which probably resulted from crack initiation associated with compression buckling. Piers with high axial loads failed as a result of fracture of one or more spirals.

P-Δ effects can reduce the lateral load carrying capacity of piers significantly as well as the displacement at which the tangential lateral stiffness becomes negative. It is important to recognise these effects in ductile design.

The length of the regions of plasticity increase both with increasing aspect ratio and with axial load ratio. The location of the plastic hinge is close to the base of the pier for low axial loads, but rises from 1.5D (D = the pier diameter) for low axial loads to 2.5D for high axial loads.

Displacement ductilities greater than the design value of six were easily achieved. Average section curvature ductilities of over 30 were measured.

Dynamic response of material behaviour and to some extent the inability to accurately measure the properties of the material, indicate that adequate over-strength factors for capacity design must be used. Over-strengths of 20% were common in these dynamic tests. These over-strengths are based on calculating the nominal flexural strengths from factored ACI equations.

5 ACKNOWLEDGEMENTS

The authors wish to acknowledge the financial contributions made to this project by Transit New Zealand (formerly New Zealand National Roads Board). We also wish to acknowledge the willing effort and expertise of the technical staff of the Civil Engineering Department of the University of Canterbury in contributing to the success of this project.

6 REFERENCES

American Concrete Institute. 1983. Building Code requirements for reinforced concrete. ACI318-83, Detroit, USA.

Dodd, L.L. 1992. The dynamic behaviour of bridge piers subjected to New Zealand seismicity. Ph.D. Thesis. Civil Engineering Department, University of Canterbury, Christchurch, New Zealand.

Dodd, L.L. and Cooke, N. 1991. Dynamic response of reinforced concrete bridge piers. Pacific conference on earthquake engineering. Nov. 1991. Auckland, New Zealand.